

Available online at [www.sciencedirect.com](http://www.sciencedirect.com)**SciVerse ScienceDirect**

Procedia Engineering 60 (2013) 195 – 200

**Procedia  
Engineering**[www.elsevier.com/locate/procedia](http://www.elsevier.com/locate/procedia)6<sup>th</sup> Asia-Pacific Congress on Sports Technology (APCST)

## Novel biosensor for Interleukin-6 detection

Jingfeng Huang<sup>a,b</sup>, James Harvey<sup>c</sup>, Derrick Fam W. H.<sup>a</sup>, Myra A. Nimmo<sup>c</sup>, Alfred Tok I.Y.<sup>a,b,\*</sup><sup>a</sup> School of Materials Science and Engineering, Nanyang Technological University, 50 Nanyang Avenue, Singapore 637553<sup>b</sup> Institute for Sports Research, Nanyang Technological University, 50 Nanyang Avenue, Singapore 639798<sup>c</sup> School of Sport, Exercise and Health Sciences, Loughborough University, Ashby Road, Loughborough, LE11 3TU, UK

Received 20 March 2013; revised 6 May 2013; accepted 9 May 2013

### Abstract

Interleukin-6 (IL-6) is a pleiotropic cytokine with an important role in both immune regulation and exercise metabolism. During exercise, IL-6 is predominantly produced within, and released from, the working skeletal muscle, with the magnitude of IL-6 release related to the duration and intensity of the exercise bout. IL-6 (a) is the first cytokine to appear in circulation following initiation of exercise and (b) undergoes the most pronounced increase as compared to any cytokine in response to exercise. In the last decade, studies have suggested a role for IL-6 as a muscle energy sensor, pointing to its potential role as a biomarker of overtraining. Currently, ELISA and western blot is the staple detection technique for IL-6. However, they require substantial time, cost, machinery and specialist training. On the other hand, a Graphene Oxide-based amperometric sensor can provide real-time, low-cost yet sensitive protein detection. But, the coverage of mono-layered Graphene Oxide (GO) flake on SiO<sub>2</sub> substrate is limited due to rinsing and unwanted crosslinking of the 3-AminoPropylTriEthoxy Silane (APTES) adhesion layer, thus leading to low available GO surface area, high variability of electrical conductivity between chips and low sheet transconductance that limits sensitivity of the sensor. This work had overcome this limitation by depositing carbon on the edges of GO flakes using an ethanol chemical vapor deposition (CVD). Then, the post-treated GO is fabricated into a liquid-gated biosensor and the detection window for IL-6 is presented. Our work yielded a highly conductive and electrically homogeneous carbon-based transducer to enable low-cost, facile, real-time yet sensitive amperometric sensors for IL-6.

© 2013 The Authors. Published by Elsevier Ltd. Open access under [CC BY-NC-ND license](https://creativecommons.org/licenses/by-nc-nd/4.0/).

Selection and peer-review under responsibility of the School of Aerospace, Mechanical and Manufacturing Engineering, RMIT University

**Keywords:** Interleukin-6; reduced graphene oxide growth; chemical vapor deposition; biosensor, liquid-gated field effect transistor

\* Corresponding author. Tel.: +65-7904935; fax: +65-6790 9081.

E-mail address: [miytok@ntu.edu.sg](mailto:miytok@ntu.edu.sg).

## 1. Introduction

Interleukin-6 (IL-6) is an important pleiotropic cytokine, which is reported to have both pro- and anti-inflammatory effects [1, 2]. During acute exercise, IL-6 is released from the working skeletal muscle, with changes in plasma IL-6 levels detectable after 30 minutes of treadmill running[3]. IL-6 levels increase as a function of the intensity and duration of the exercise bout, with duration accounting for more than 50% of the variation in circulating IL-6 levels[4]. This increase is not linear, but rather follows a near-exponential pattern: plasma IL-6 concentrations have been reported to increase more than 100-fold after a marathon [5], while more modest increases are usually observed[4]. In extreme cases, such as ultramarathon running, IL-6 levels reach those only seen in severe sepsis, with an 8000-fold increase reported in finishers of the 246 km Spartathlon race[6]. IL-6 levels peak at the cessation of exercise, or shortly thereafter, followed by a rapid decrease to baseline levels [3, 4]. This is followed by the induction of an anti-inflammatory cytokine profile, with increases in circulating IL-1 receptor agonist (IL-1ra), IL-10 and cortisol levels [5, 7].

Studies [8, 9] have reported the detection of IL-6 in the sweat of healthy premenopausal women, and those with Major Depressive Disorder (MDD), using Recycling Immunoaffinity Chromatography (RIC). In this detection method, samples pass through a succession of affinity columns. In RIC studies on human sweat [8, 9], subjects wore sweat patches for 24 hours – plasma and sweat IL-6 levels were found to correlate, with no significant differences between IL-6 levels in each fluid. These studies therefore present interesting theoretical grounding for developing non-invasive IL-6 sensor technology.

From a review of literature, no group has reported the electrical detection of IL-6 using graphene or reduced graphene oxide. Currently, ELISA or western blotting is the staple for detection of IL-6. These techniques require substantial time, machinery and specialist training. The same is true of the RIC method used for analysis of sweat samples. In comparison, low-cost Graphene Oxide-based amperometric Field Effect Transistor (FET) sensors allow for facile analyte detection, while remaining highly-sensitive. However, the coverage of mono-layered Graphene Oxide flake on SiO<sub>2</sub> substrate is limited to ca. 60-90% due to rinsing and unwanted cross-linking of 3-AminoPropylTriEthoxy Silane (APTES) adhesion layer. This partial coverage of Graphene Oxide leads to low and large variability in electrical conductivity that limits the sensitivity of the sensor. In this paper, we show a technique of novel post-processing of Graphene Oxide which can fill the whole chip and homogenize the carbon, yielding a low-cost and facile platform suitable for sensitive detection of IL-6. Finally, we present the detection window for IL-6.

## 2. Experimental

Graphite flakes of 3-5mm were obtained from NGS Naturgraphit GmbH, Germany. All the chemicals (research grade) were obtained from Sigma Aldrich and Merck. IL-6 protein and antibody were obtained from BD (ELISA kit No. 555220). Graphene oxide (GO) sheets were prepared by the modified Hummers' method from natural graphite flakes as reported [10, 11]. Briefly, graphite flakes were pre-oxidized using ultra-sonication and then oxidized using H<sub>2</sub>SO<sub>4</sub> (120ml) and KMnO<sub>4</sub> (15g). Then H<sub>2</sub>O<sub>2</sub> (20ml) was added into the mixture. Finally, the resulting floating GO particles were scooped out and stirred overnight in DI water (500ml) to obtain a stock solution of GO. This solution was then centrifuged at 3000xg for 5 minutes and further purified by dialysis (cutoff 3000MW) against DI water for one week.

Then, silicon dioxide chips were silanized using APTES and the GO solution was drop-cast. The silanization enabled a mono-layer of GO to be electrostatically attached. The chips were then placed in an atmospheric pressure ethanol CVD furnace and processed at 950°C. In the CVD, H<sub>2</sub> (20scm) and Ar (100scm) gas are mixed and passed through an ethanol bubbler before entering the furnace. Finally, the

chip was then fabricated into a liquid-gated FET biosensor with 1-pyrenebutanoic acid, succinimidyl ester (PBSE) linker, IL-6 antibody with blocking agents bovine serum albumin and ethanolamine.

### 3. Results and discussion

According to Lerf-Klinowski's graphene oxide model, carboxyl (-COOH) groups are found at the edges of GO[12-14]. Thus an etching action by  $H_2$  is added to activate the carbon sites, followed by possible carbon deposition at the edges. Scanning Electron Microscopy (SEM) is performed and the image of GO before growth (Figure 1a), after a 30-minute CVD treatment growth (Figure 1b) and a high magnification image of the carbon growth observed near the edges of GO (Figure 1c) are shown. In the images, the GO flakes are highlighted in purple and the new carbon growths are highlighted in yellow. Since we observed no carbon growth using clean wafer substrates and no carbon growth on  $SiO_2$  has been reported, the carbon deposition must be due to carbon deposition initiated by the initial GO flake.

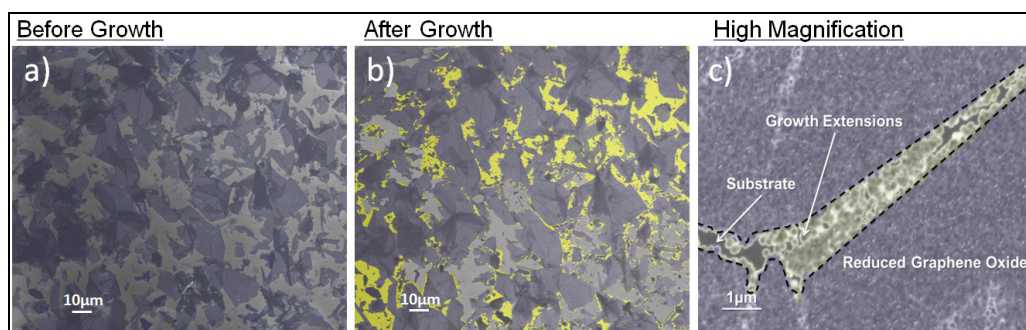


Fig. 1. SEM images of (a) GO flakes before ethanol CVD treatment with ca. 60% coverage (b) reduced GO flakes after 30-minutes CVD treatment with ca. 75% coverage in total. (c) high-magnification on the new growths between two reduced GO flakes. [GO flakes and new carbon growths are highlighted in purple and yellow respectively]

An optical image of a 2-hour ethanol CVD processed chip is shown in Figure 2a. It is observed that after 2-hour ethanol CVD treatment, the carbon new growth completely covers the silicon dioxide substrate. This is shown in a Raman mapping in Figure 2b. 2-D peak ( $\sim 2700\text{cm}^{-1}$ ) that is characteristic of graphene is observed on and out of pre-existing GO flake as shown in Figure 2c. It is reported that an up-shift in the Raman 2D peak position corresponds to an increase in the number of graphene layers [15]. From the Raman map, the overall growth of the substrate is 100%.

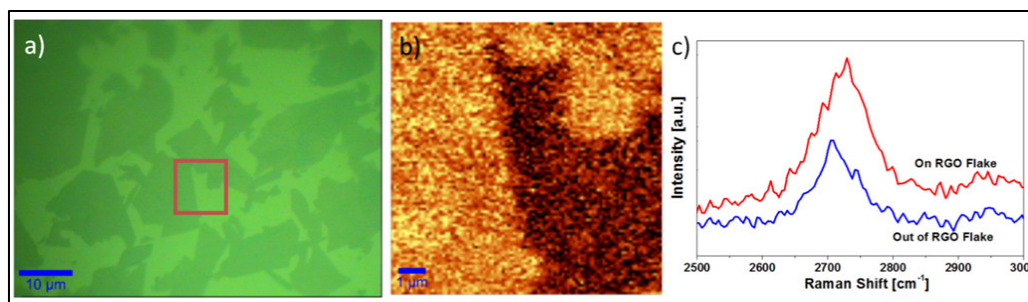


Fig. 2. (a) Optical microscope image of 2-hour processed reduced GO flakes on  $SiO_2$  substrate (b) Raman mapping at edges of RGO flakes showing 100% carbon coverage. (c) Raman spectrum of both on and out of RGO flakes.

GO on SiO<sub>2</sub> substrates were treated with 15, 60 and 120 minutes of ethanol CVD and hydrazine vapour (n=5). The electrical resistivity was then measured with a 4-point probe and presented in Table 1. The average electrical resistance after 15 minutes of ethanol CVD treatment is 2 magnitudes less than the hydrazine reduced samples, due to improved graphitization. However, the standard deviation only decreases marginally by 9.8%. As the ethanol CVD process time increased to 2 hours, the standard deviation decreased dramatically by 79.5% while the electrical resistance also decreased by 79.5% compared to the hydrazine reduced samples. The resistance drop and standard deviation decrease could be due to the complete 100% carbon coverage of the sample chips, as shown in SEM and the Raman map.

Table 1. Electrical measurements of reduced GO processed under different conditions

Reduction Conditions	Hydrazine Vapor Reduction		Ethanol CVD Reduction	
	12 hours	15 mins	1 hour	2 hours
Average Resistance ( $\Omega/T$ )	1.99E+06	6.10E+04	2.23E+04	4.68E+03
Absolute Standard Deviation ( $\Omega$ )	1.60E+06	4.42E+04	7.14E+03	7.70 +02
Relative Standard Deviation (%)	80.5	72.6	32.1	16.5

To test the reduced GO electrical properties, back-gated FETs based on 2-hours ethanol CVD processed GO sheets were fabricated and their electrical properties tested under ambient temperature and pressure. The channel length was 100 $\mu$ m to ensure transport is bulk-limited and the role of the all contacts minimized. Figure 3a shows the drain current ( $I_d$ ) versus drain voltage ( $V_d$ ) curve prepared with ethanol CVD processed reduced GO FET at six discrete gate voltages ( $V_g$ ). The  $I_d$ – $V_d$  graph shows linear output behaviour indicative of a good ohmic contact between the GO film and electrodes. Figure 3b illustrates the same transistor  $I_d$  under sweeping  $V_g$  at fixed  $V_d=0.1V$ . The threshold voltage is shifted to the positive side due to p-doping from atmospheric moisture and oxygen. The device showed a clear increase in conductance as the gate voltage changed from +100V to -100V, indicating that the reduced GO films behaved as a p-type semiconducting material.

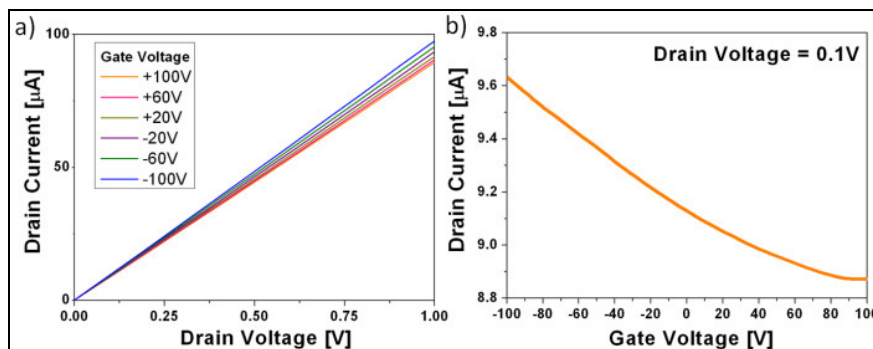


Fig. 3. (a)  $I_d$ – $V_d$  output characteristics under different applied  $V_g$  (b)  $I_d$ – $V_g$  transfer curve of the ethanol CVD-processed reduced GO transistor device.

The ethanol CVD-treated reduced GO chips were then fabricated into liquid gated FETs in order to test their bio-sensing capability. As shown in Figure 4a, gate voltage applied via the reference electrolyte, shifted the reduced GO Fermi level and resulted in a conductance change. When the Fermi level crosses

over the Dirac point ( $V_D$ ), the majority charge carrier is changed and lead to ambi-polar behavior [16]. For liquid gating, two transport regimes are observed on both sides of the Dirac point, the hole ( $V_g < V_D$ ) and electron ( $V_g > V_D$ ) regime. The minimum current with sweeping  $V_g$  is the Dirac point and is observed at  $V_g = +230\text{mV}$ . This shift in Dirac point is due to substrate-induced doping. As every FETs will have varying Dirac point due to persistent doping, the gate voltage is fixed at  $+400\text{mV}$  for subsequent bio-sensing experiments.

The isoelectric point of IL-6 is approximately 4~5.3 and the pH of the buffer used is 7.4. Hence IL-6 possesses a net negative charge. At measurement of  $V_g = +400\text{mV}$ , binding of IL-6 to the antibody modified GO surface would induce a consequential decrease in conductance because of the n-type conducting regime of the GO ( $V_g > V_D$ ) as shown in Figure 4b. The sensor response correlated to the conductance change before and after protein bound to the functionalized GO surface. It was found that the fabricated chip is stable in an aqueous environment for more than 4 hours. The results show that GO-based transducers with antibody can sense for clinical relevant quantities down to  $4.7\text{pg/ml}$ .

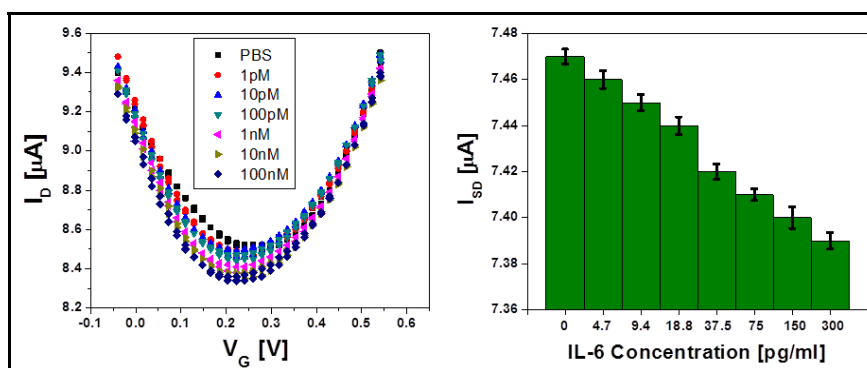


Fig. 4. (a) Drain current vs. gate voltage curve obtained with different concentration of IL-6 concentrations. (b)  $I_{SD}$  characteristic measurement with different clinically relevant concentrations of IL-6 protein at fixed gate voltage.

Previous studies have reported resting IL-6 levels of  $\sim 10\text{pg/ml}$  in sweat samples from healthy women [8, 9]. These values were demonstrated not to be significantly different from plasma levels ( $p = 0.19$ ; [8]). The ranges reported in the control group for each study were within the detection limit of this sensor. However, other studies on physically active subjects have reported resting plasma IL-6 levels of  $\leq 1\text{pg/ml}$  [5, 17]. In light of this, further work will be required to improve the detection limit of the sensor further. Nonetheless, we believe this research provides a promising starting point for future development of highly-sensitive, real-time IL-6 detection.

#### 4. Conclusion

We have successfully demonstrated that a post-treatment ethanol chemical vapor deposition of graphene oxide can be utilized to increase the coverage of Graphene Oxide to 100%, lower the electrical resistivity deviation between chips by 79.5% and demonstrated it for bio-sensitive sensing for Interleukin-6 (IL-6) down to the body physiological-relevant range. Finally, we believe that the results from this experiment will support both the research of IL-6 and carbon biosensors with this facile, low-cost, real-time bio-sensor.

## Acknowledgements

The authors are grateful for the funding from the Institute for Sports Research (ISR) of Nanyang Technological University (NTU). The research was also partly supported by the National Institute for Health Research (NIHR) Diet, Lifestyle & Physical Activity Biomedical Research Unit based at University Hospitals of Leicester and Loughborough University. The views expressed are those of the authors and not necessarily those of the NHS, the NIHR or the Department of Health.

## References

- [1] Scheller J, Chalaris A, Schmidt-Arras D, Rose-John S, The pro- and anti-inflammatory properties of the cytokine interleukin-6. *Biochimica et biophysica acta* 2011; **1813** 878-888.
- [2] Leggate M, Nowell MA, Jones SA, Nimmo MA, The response of interleukin-6 and soluble interleukin-6 receptor isoforms following intermittent high intensity and continuous moderate intensity cycling. *Cell stress & chaperones* 2010; **15** 827-833.
- [3] Ostrowski K, Rohde T, Zacho M, Asp S, Pedersen BK, Evidence that interleukin-6 is produced in human skeletal muscle during prolonged running. *The Journal of Physiology* 1998; **508** 949-953.
- [4] Fischer CP, Interleukin-6 in acute exercise and training: what is the biological relevance? *Exercise immunology review* 2006; **12** 6-33.
- [5] Ostrowski K, Rohde T, Asp S, Schjerling P, Pedersen BK, Pro- and anti-inflammatory cytokine balance in strenuous exercise in humans. *J Physiol* 1999; **515 ( Pt 1)** 287-291.
- [6] Margeli A, Skenderi K, Tsironi M, Hantzi E, Matalas A-L, Vrettou C, et al., Dramatic Elevations of Interleukin-6 and Acute-Phase Reactants in Athletes Participating in the Ultradistance Foot Race Spartathlon: Severe Systemic Inflammation and Lipid and Lipoprotein Changes in Prolonged Exercise. *Journal of Clinical Endocrinology & Metabolism* 2005; **90** 3914-3918.
- [7] Steensberg A, Fischer CP, Keller C, Møller K, Pedersen BK, IL-6 enhances plasma IL-1ra, IL-10, and cortisol in humans. *American Journal of Physiology - Endocrinology And Metabolism* 2003; **285** E433-E437.
- [8] Marques-Deak A, Cizza G, Eskandari F, Torvik S, Christie IC, Sternberg EM, et al., Measurement of cytokines in sweat patches and plasma in healthy women: validation in a controlled study. *Journal of immunological methods* 2006; **315** 99-109.
- [9] Cizza G, Marques AH, Eskandari F, Christie IC, Torvik S, Silverman MN, et al., Elevated neuroimmune biomarkers in sweat patches and plasma of premenopausal women with major depressive disorder in remission: the POWER study. *Biological psychiatry* 2008; **64** 907-911.
- [10] Larisika M, Huang J, Tok A, Knoll W, Nowak C, An improved synthesis route to graphene for molecular sensor applications. *Materials Chemistry and Physics* 2012; **136** 304-308.
- [11] Huang J, Larisika M, Fam WHD, He Q, Nimmo MA, Nowak C, et al., The extended growth of graphene oxide flakes using ethanol CVD. *Nanoscale* 2013; **5** 2945-2951.
- [12] Szabó T, Berkesi O, Forgó P, Josepovits K, Sanakis Y, Petridis D, et al., Evolution of Surface Functional Groups in a Series of Progressively Oxidized Graphite Oxides. *Chemistry of Materials* 2006; **18** 2740-2749.
- [13] Cai W, Piner RD, Stadermann FJ, Park S, Shaibat MA, Ishii Y, et al., Synthesis and Solid-State NMR Structural Characterization of <sup>13</sup>C-Labeled Graphite Oxide. *Science* 2008; **321** 1815-1817.
- [14] Boukhvalov DW, Katsnelson MI, Modeling of Graphite Oxide. *Journal of the American Chemical Society* 2008; **130** 10697-10701.
- [15] Eda G, Fanchini G, Chhowalla M, Large-area ultrathin films of reduced graphene oxide as a transparent and flexible electronic material. *Nat Nano* 2008; **3** 270-274.
- [16] Hess LH, Jansen M, Maybeck V, Hauf MV, Seifert M, Stutzmann M, et al., Graphene Transistor Arrays for Recording Action Potentials from Electrogenic Cells. *Advanced Materials* 2011; **23** 5045-5049.
- [17] Bruunsgaard H, Galbo H, Halkjaer-Kristensen J, Johansen TL, MacLean DA, Pedersen BK, Exercise-induced increase in serum interleukin-6 in humans is related to muscle damage. *J Physiol* 1997; **499 ( Pt 3)** 833-841.